

A Four Parameter Fitting Method to Quantify Fully the Sources of Phase Contrast in Gradient Echo MRI

S. Wharton¹, and R. Bowtell¹

¹Sir Peter Mansfield Magnetic Resonance Centre, University of Nottingham, Nottingham, United Kingdom

Introduction: Phase images of the human brain acquired using gradient echo techniques show excellent contrast at high field [1]. Until recently, this contrast was thought to be entirely due to spatial variation of the NMR frequency resulting from differences in the isotropic magnetic susceptibility of tissues. Recently, however, three additional contrast mechanisms that could potentially contribute to phase contrast in human brain tissue have been proposed. These are: (i) frequency offsets due to exchange processes [2]; (ii) field perturbations due to oriented NMR-invisible microstructures [3]; (iii) anisotropy of the magnetic susceptibility [4]. Here, we present a method for fitting and separating the contributions of each of the four proposed contrast mechanisms using MRI phase data acquired with the sample at multiple orientations to the main magnetic field, B_0 , in combination with diffusion tensor imaging data (DTI) acquired at a single orientation. The operation of the fitting methodology is demonstrated using simulated data from a numerical phantom. The proposed approach could simplify the interpretation of phase contrast and give researchers access to a plethora of new contrast information.

Theory: The fitting process involves the weighted least squares minimisation of a cost function formed from a combination of functions related to field map measurements made at multiple orientations to B_0 , and a set of data masks, as shown in Eq.1. For each proposed contrast mechanism there is an associated spatially varying parameter: isotropic susceptibility = χ_{iso} , exchange = E_{oi} , microstructure = H_{mstr} , and anisotropy = χ_{aiso} . There is also an associated forward calculation (FC) for simulating the field map due to the spatial distribution of each parameter. For χ_{iso} the FC involves convolution with the dipole field kernel [5] which yields a field map that depends on the angle, $\theta_{k,j}$, between \mathbf{k} and B_0 for each orientation, O_j (Eq.3). For E_{oi} the FC is simply a point-wise multiplication with a mask that defines the signal-generating region, $M_{s..}$. This yields a local field shift that is independent of orientation (Eq. 4). For H_{mstr} the FC is a point-wise multiplication with a dipole field term [3] that is dependent on the angle, $\theta_{D,j}$, between B_0 and the axis describing the orientation of microstructure within each voxel (Eq.5). The axis of the microstructure could be identified through use of DTI techniques [6]. For χ_{aiso} the FC is more complicated. A 6 parameter fit is needed to define the full anisotropic susceptibility tensor [4]. Here, we make 3 assumptions to simplify the FC to a function of a single anisotropy parameter, χ_{aiso} . These are: (i) the tensor describing the anisotropy is cylindrically symmetric (CS), a valid assumption when considering samples with cylindrical geometry, such as white matter (WM) fibres; (ii) the orientation of the principal axis of the susceptibility tensor is known (e.g. from DTI); (iii) the CS tensor has zero trace. This is a valid assumption because the mean susceptibility is fitted and removed through χ_{iso} . Making these assumptions the FC for χ_{aiso} is given by Eq.6, where $\theta_{T,j}, \phi_{T,j}$ define the principal axis of the CS tensor relative to B_0 , while $\theta_{k,j}, \phi_{k,j}$ are the spherical coordinates of \mathbf{k} relative to B_0 . These convolutions yield a non-local field map dependent on the sample's orientation with respect to B_0 . The susceptibility along the principal axis is given by $\chi_{aiso} + \chi_{iso}$, and the two orthogonal and equal (assuming CS) susceptibilities are given by $\chi_{iso} - \chi_{aiso}/2$. By utilising these FC's the contrast parameters can be fitted by simulating field maps (Eq.3-6) and comparing their sum to scaled phase data, ΔB_j , (Eq.2) acquired at multiple, N_o , orientations, $j=1-N_o$, to B_0 , see Eq.1. The fitting can be achieved via a conjugate gradient algorithm. The weighting, W , can be formed from a mask of the signal-generating volume or a measure of the inverse variance of the phase measurement, which can be estimated from the MRI modulus data. To improve the fitting, masking terms, $M_{iso}...$ etc (Eq.1), are included in order to inform the algorithm about null regions where each parameter is known to be zero. For χ_{iso} and E_{oi} the masks, M_{iso} and M_{oi} , are the signal-generating voxels. For H_{mstr} and χ_{aiso} , DTI information could provide a measure of the validity of the orientation information used in the FC's. For example, FA values [6], could be used to form more restricted masks, M_{mstr} and M_{aiso} , that exclude voxels in which there is no measurable orientation.

Methods: A numerical phantom containing 5 ellipsoids was created (Fig.1a). Four were each populated with one of the different contrast parameters, while a 5th composite ellipsoid was populated with a mixture of all 4 contrast parameters. The relative magnitudes of each parameter were set to give an approximately equal average contribution to the field maps over all the orientations, these were chosen as: $\chi_{iso}=1$, $E_{oi}=1/6$, $H_{mstr}=1/3$, and $\chi_{aiso}=1$. The composite ellipsoid had the same relative contributions from each parameter divided by a factor of 4. To provide a rigorous test of the fitting procedure, the axis of orientation was set to two different values within each ellipsoid containing H_{mstr} and χ_{aiso} , half of each ellipsoid had an axis of orientation along the z -axis and the other half had an axis oriented along y . Fig.1b&c shows the field maps produced from the numerical phantom for two different B_0 orientations. Parameter maps were fitted based on field maps simulated with B_0 at 13 different orientations, approximately evenly spread over a hemi-spherical surface. A realistic level of Gaussian noise was added to each field map (with standard deviation/mean = 0.01/0) and the conjugate gradient algorithm was limited to 100 iterations. The masks were chosen for each parameter as discussed above, and are shown in Fig.2a-d.

Results: Fig.2.e-h shows the fitted parameter maps. The reconstructed parameter maps were found to be accurate with an error of less than 1% when averaged over each ellipsoid. The parameter maps for the composite ellipsoid showed a higher variance relative to the other ellipsoids, consistent with the lower SNR value (1/4 of outer). In conclusion, we have presented a method for inverting field maps measured at multiple orientations to B_0 to calculate the contributions of the 4 proposed phase contrast mechanisms. The methodology assumes *a priori* knowledge of the axis of orientation of microstructure and cylindrically symmetric susceptibility anisotropy, as well as a measure of the validity of this information. For human brain imaging this information is readily available through DTI techniques making the methodology presented here applicable for clinical MRI.

References:[1] Duyn et al. 2007. PNAS.104:11796-11801, [2] Zhong et al. 2008. NIMG. 40:1561-1566, [3] He et al. 2009. PNAS.106:13558-13563, [4] Liu, C. 2010. MRM. 63:1471-1477, [5] Marques et al. 2005. CMR PB MRE. 25B,65-78, [6] Mori et al. 2006. AJNR. 27:1384-1385.

$$\min_{\chi_{iso}, E_{oi}, H_{mstr}, \chi_{aiso}} \left(\|O_1\|_2^2 + \|O_2\|_2^2 + \|O_3\|_2^2 + \|O_4\|_2^2 + \dots + \|O_N\|_2^2 \right) \quad \text{Eq.1}$$

$$+ \alpha \|M_{iso} \chi_{iso}\|_2^2 + \alpha \|M_{oi} E_{oi}\|_2^2 + \alpha \|M_{mstr} H_{mstr}\|_2^2 + \alpha \|M_{aiso} \chi_{aiso}\|_2^2$$

$$O_j = W_j (C_{iso,j} \chi_{iso} + C_{oi} E_{oi} + C_{mstr,j} H_{mstr} + C_{aiso,j} \chi_{aiso} - \Delta B_j) \quad \text{Eq.2}$$

$$C_{iso,j} \chi_{iso} = FT^{-1} (FT(\chi_{iso}) \times (\cos^2 \theta_{k,j} - 1/3)) \quad \text{Eq.3}$$

$$C_{oi} E_{oi} = M_s \times E_{oi} \quad \text{Eq.4}$$

$$C_{mstr,j} H_{mstr} = (\cos^2 \theta_{D,j} - 1/3) \times H_{mstr} \quad \text{Eq.5}$$

$$C_{aiso,j} \chi_{aiso} = FT^{-1} (FT(\chi_{aiso} (1 + 3 \cos 2\theta_{T,j})/4) \times (\cos^2 \theta_{k,j} - 1/3) + FT(3 \chi_{aiso} \sin 2\theta_{T,j} \cos \phi_{T,j}/4) \times (\sin 2\theta_{k,j} \cos \phi_{k,j})/2 + FT(3 \chi_{aiso} \sin 2\theta_{T,j} \sin \phi_{T,j}/4) \times (\sin 2\theta_{k,j} \sin \phi_{k,j})/2) \quad \text{Eq.6}$$

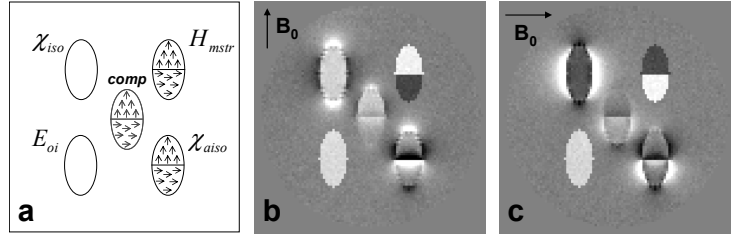


Fig1. Schematic of numerical phantom (a), and simulated field maps produced for two different B_0 orientations: parallel to z-axis (b), and parallel to y-axis (c).

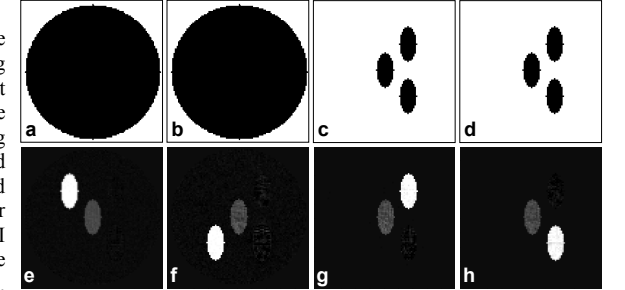


Fig2. Masks of null regions for χ_{iso} (a), E_{oi} (b), H_{mstr} (c), and χ_{aiso} (d). Also shown are the fitted values of χ_{iso} (e), E_{oi} (f), H_{mstr} (g), and χ_{aiso} (h).